ELSEVIER

Journal of Power Sources 113 (2003) 72–80

JOURNAL OF POWER SOURCES

www.elsevier.com/locate/jpowsour

Simulation of capacity fade in lithium-ion batteries

R. Spotnitz*

Battery Design Co., 2277 DeLucchi Dr., Pleasanton, CA 94588, USA

Received 26 August 2002; accepted 10 September 2002

Abstract

The technical literature, including datasheets from battery manufacturers, is reviewed to identify the major characteristics of capacity fade: impedance growth and capacity loss. Impedance growth is significant at both the positive and negative electrodes, though capacity fade loss due to SEI growth is usually attributed to the negative. Techniques for accelerated life testing are summarized. Simple models are used to describe mechanisms for capacity loss at the negative. Finally, numerical simulations are used to explore the effect of porous electrodes on fade behavior.

Keywords: Simulation; Capacity fade; Lithium-ion battery

1. Introduction

Capacity fade refers to the loss in discharge capacity that a battery demonstrates over time. The loss in discharge capacity occurs whether the battery is inactive (so-called ''calendar life'' losses) or exercised (''cycle life'' losses). The capacity loss can consist of irreversible and reversible components. Reversible capacity loss, called ''self-discharge'', can be recovered by charging the battery. Irreversible capacity loss is associated with degradation of the battery and cannot be recovered. The amount of irreversible capacity considered acceptable depends on the application of the battery.

The acceptable amount of irreversible capacity loss varies widely depending on the application. In consumer electronics, such as personal computers and cellular phones, batteries are typically expected to last a year or two. So, an irreversible capacity loss of >20% over 1–2 years would be acceptable for batteries used in many small, portable electronic devices. On the other hand, a satellite battery might be required to retain 80% of its initial capacity after 18 years or more. Automakers [1] have set a 15 years life as a goal for batteries in hybrid and full electric vehicles. Utility load leveling and telecommunications back-up batteries also require long lives. As commercial lithium-ion technology is only 11 years old, and is evolving at a rapid pace, there are no data available on the capacity fade of lithium-ion batteries over such extended periods. Nor is it practical to carry out real-time testing of batteries to qualify them for aerospace or automotive applications. Thus, there is interest in developing accelerated test methods as well as models based on a physical understanding of the causes of capacity fade. An earlier review [2] categorized possible causes of capacity fade; in contrast, this review describes work done to characterize capacity fade, methods for accelerated testing, and, lastly, models for capacity fade.

2. Manufacturer's information on capacity fade

Over the years, many battery manufacturers have reported cycle life data and some have even reported calendar life data. Fig. 1 highlights the features of a very general capacity versus cycle number plot. The shape is reminiscent of a discharge curve (voltage versus capacity), and necessarily so. The rate of capacity decrease is initially high (region A), but slows quickly (region B) and, after a few hundreds of cycles, slows again (region C) before starting a rapid increase (region D). End of life, defined as when the battery reaches 80% of its initial capacity, usually occurs in region C, so battery manufacturers do not publicly report data for region D. The capacity fade from regions A through C is often indistinct and so approximated as linear and expressed in terms of percentage capacity loss per cycle. Fig. 2 shows typical voltage curves for charge and discharge [3]. As the cell cycles, the ohmic resistance increases pushing the discharge curve down to lower voltages and the charge curve up to higher voltages. As a consequence, the 4.2 V

* Tel.: +1-925-895-4080; fax: +1-925-600-9812.
E-mail address: rspotnitz@batdesign.com (R. Spotnitz).

0378-7753/02/$ – see front matter
PII: S0378-7753(02)00490-1

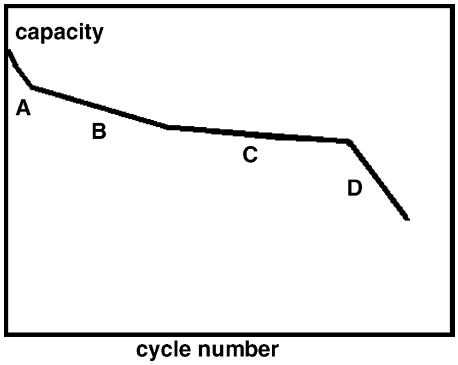

Fig. 1. General shape for capacity versus cycle number plots.

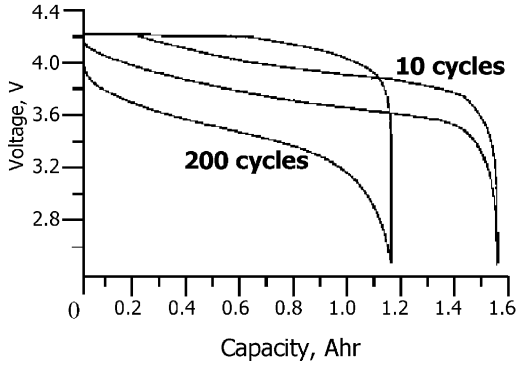

Fig. 2. Effect of cycle number on charge/discharge voltage profile [3].

limit on charge is reached earlier in the charge step and more time is spent at 4.2 V. Referring to Fig. 2, after 200 cycles, a cut-off voltage on discharge of 3.0 V gives 1.08 Ah versus 1.18 Ah for a cut-off voltage of 2.5 V, whereas, after 10 cycles there is no significant difference in discharge capacity for the two cutoff voltages. Pure ohmic drop does not account for all the capacity loss on cycling as, at the end of discharge, the curve shows a characteristic drop indicating depletion of active material. Fig. 3 shows a typical shape for calendar life (capacity versus time) data that is reported by battery manufacturers. As time proceeds, the rate of capacity loss decreases. The capacity loss during calendar life testing exhibits reversible and irreversible components. Part of the capacity loss can be recovered by charging the

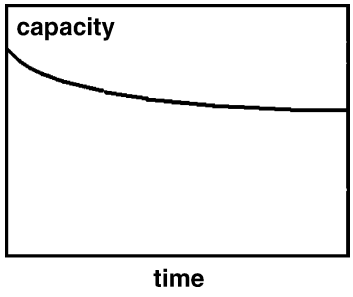

Fig. 3. Typical capacity versus time for storage test.

cell; however, the shape of the capacity retention versus time (Fig. 3) is similar regardless of whether capacity refers to capacity after storage (both irreversible and reversible loss) or capacity after storage and charging (irreversible loss only).

Sony Corporation, which was the first to commercialize lithium-ion technology in 1991, has introduced many different types of lithium-ion batteries over the years. Sony originally produced lithium-ion cells with negative electrodes consisting of hard carbon and positive electrodes consisting of lithium cobalt oxide. Later Sony added cells with graphite negatives and even, at one time, offered a cell with a $LiNiO_2$ positive.[1] Sony offers cells in cylindrical, prismatic, and soft packages. For all the cell types the range of capacity loss at 500 cycles varies from 12.4% (US18650, $LiCoO_2$/hard carbon) to 24.1% (US18650G3, $LiCoO_2$/graphite), corresponding to an average capacity loss per cycle range of 0.025–0.048% per cycle. However, for each of the cells, only a single data set was given, so it is not possible to gauge how significant the differences are between the cell types. In a Sony technical manual, the range of capacity loss for the US18650 cell type at 500 cycles varies from ∼10 to 18% [4]. Cycle life results extracted from NEC Moli (now obsolete) datasheets suggest that cobalt oxide cells provides lower capacity fade than manganese oxide cells. Data extracted from Panasonic datasheets indicate that graphite cells can be made with the low levels of capacity loss obtained with Sony hard carbon cells; the Panasonic data also suggest there are no significant differences in capacity loss between prismatic and cylindrical cells.

Sony has reported the effect of state-of-charge (SOC) on irreversibility capacity loss at 20 and 40 °C (see Table 1) [4]. The irreversible capacity loss increases dramatically with increasing SOC and with increasing temperature; when stored at 40 °C and 100% SOC the battery loses ∼30% of its initial capacity in 1 year. In view of the cycling data (Table 1) these results indicate that the irreversible capacity loss due to storage (11% after 0.25 years at 20 °C) is comparable to the capacity loss due to cycling (12% after 500 cycles, ∼0.3 years at 23 °C).

Toshiba's literature [5] has provided capacity fade on cycling and on storage for their $LiCoO_2$/graphite chemistry. On cycling, the fade rate is 0.024% per cycle or 12% after 500 cycles (which takes ∼0.2 years) at 20 °C. On storage at 4.2 V, the capacity loss appears to be linear with time and increases with increasing temperature. At 20 °C after 3 months, the irreversible capacity loss is only about 3%, so the capacity loss due to storage is small relative to loss due to cycling. These data, with $LiCoO_2$/graphite cells, are very different than the Sony data with $LiCoO_2$/hard carbon cells where storage losses are much greater than cycling losses. Toshiba's literature gives the irreversible capacity loss versus time at 20, 40 and 60 °C. The slopes of the

[1] The US14500N was listed on Sony's website a few years ago, but is no longer.

Table 1
Irreversible loss of discharge capacity for Sony US18650 cells after storage for 1 year (estimated from charts) [3]

State-of-charge	Years at 20 °C[a]			Years at 40 °C[a]		
	0.25	0.5	1.0	0.25	0.5	1.0
0% (~3.2 V)	0	0	0	0	0	0
50% (~3.85 V)	5	6	6	6	10	11
100% (~4.2 V)	11	14	17	19	26	30

[a] Irreversible capacity loss (%).

irreversible capacity loss versus time plots follow Arrhenius behavior, so Toshiba's data can be expressed as

$$\%\,\text{capacity loss} = 1.544 \times 10^7 \exp\left(\frac{-40498}{8.3143T}\right)t \quad (1)$$

where T (K) is the temperature and t (months) the time. The magnitude of the activation energy (40.5 kJ/mol) indicates that a chemical process is responsible for the capacity fade. Eq. (1) is an example of time/temperature superposition; it can be used to estimate calendar life (80% capacity loss) of 21 months at 20 °C even though data are only available for a 6 months period.

Panasonic [6] gives charts of cycle life at 20 °C, and storage characteristics at 20 °C and 10 months for $LiCoO_2$/graphite cells. For the CGP30486 Prismatic Cell (January 2000 datasheet), the nominal capacity is 630 mAh and the recommended charge condition is constant voltage/constant current, 4.1 V, 420 mA, 2 h, 20 °C. After 500 cycles, the cell loses ~19% of its initial capacity. After storage for 2 months in the initially, fully charged condition, about 7% of the initial capacity is lost to self-discharge, and, after 6 months, about 10% of the initial capacity is lost. However, all of the capacity lost on storage is recoverable, even up to 10 months, confirming Toshiba's result that the irreversible capacity loss due to storage is small relative to the loss due to cycling for $LiCoO_2$/graphite cells.

Plots of log(DOD) versus cycle number are linear for many aqueous battery systems [7], but lithium-ion manufacturers have not published similar data except for some results from Toshiba concerning lithium-ion button cells that show linear behavior from 20 to 100% DOD [8].

In summary, the data from lithium-ion battery manufacturers indicates that lithium-ion cells with a cycle life of 500 cycles can be produced regardless of shape (cylindrical, rectangular, soft packaging) or chemistry ($LiCoO_2$, $LiNiO_2$, $LiMn_2O_4$, graphite, hard carbon). Calendar life is adversely affected by storage in a charged state or at earlier ambient temperatures. Cycling a $LiCoO_2$/graphite cells causes capacity fade beyond that expected from calendar life losses alone.

3. Published studies of capacity fade

A number of studies have been published that characterize the capacity fade behavior of commercial cells.

Johnson and White [9] cycled a number of commercial cells and verified manufacturer's claims of cycle life. The Sony 18650 cell ($LiCoO_2$/hard carbon) was charged using a CC/CV condition of 1.0 A to 4.2 V for 2.5 h (instead of the 3 h reported by Sony) and they found a 12% capacity loss after 1000 cycles (versus 12% at 500 cycles reported by Sony, see Table 1).

Tobishima et al. [10] examined the capacity retention of commercial Sony 18650 cells (1.2 Ah capacity, $LiCoO_2$/hard carbon). In one set of experiments, cells were stored under one of four conditions (20 or 60 °C and potentiostatically at 4.1 or 4.2 V) for a period of 1 year, during which the capacity was determined monthly. For each storage condition, a semi-log plot of capacity (determined with a 1 A discharge) versus log(storage duration) produced a linear relationship. Extrapolation of the line to 10 years indicated that the cells stored at 20 °C retained 64% (4.2 V) and 80% (4.1 V) whereas the cells stored at 60 °C retained 33% (4.2 V) and 37% (4.1 V). These results indicate there is an interaction between temperature and SOC; at low temperature, increasing SOC strongly increases irreversible capacity loss, while at high temperature, increasing SOC only slightly increases irreversible capacity loss. They also examined capacity fade in cells charged to 4.2 V and allowed to stand at 20 or 60 °C. These cells lost capacity during storage; after 12 months at 20 °C, cell had 77% of initial capacity and the capacity increased to 82% on charging (this agrees very well with Sony's data, see Table 1), whereas a cell stored at 60 °C had 50% of its initial capacity, increasing to 60% after charging. Although the data are not directly comparable, the interaction between voltage and temperature reported by Tobishima et al. [10] (higher cell voltage increase capacity loss less at elevated temperature than at 20 °C) does not agree with the Sony data [4] that indicates the opposite effect (higher cell voltage increases capacity loss more at higher temperature than at 20 °C).

Wu et al. [11] used a reference electrode in an 18650-size cell to measure the impedance of both the positive (cobalt oxide) and negative (graphite) during cycling. They found the impedance of the positive, which was initially about twice that of the negative, nearly doubled after 100 cycles whereas the negative impedance increased only slightly.

Zhang et al. [12] cycled Sony 18650 lithium-ion cells (US18650S), then removed and characterized the individual electrodes using cyclic voltammetry, ac impedance, and electron probe microscopic analysis (EPMA). Nyquist plots obtained for full cells showed two intercepts with the real axis; a high frequency intercept at about 0.2 Ω that was independent of cycle number, and a second intercept at lower frequencies that increased linearly with cycle numbers from 0 to 800. Examination of the individual electrodes in the charged state after 10 cycles revealed that the impedance of cobalt oxide electrode was about 3× greater than that of the negative electrode; after 800 cycles, the impedance of the cobalt oxide electrode as about 5× greater than that of the negative electrode.

Rakotondrainibe et al. [13] evaluated several commercial lithium-ion cells for low-earth-orbit (LEO) satellite applications. They dissected cells from Sony ($LiCoO_2$/hard carbon, 18650S, 1.3 Ah), Panasonic ($LiCoO_2$/graphite, CGR 17500, 0.8 Ah), and Sanyo ($LiCoO_2$/graphite, 18650, 1.35 Ah) and found that the weight ratio of positive coating to negative coating was 2.66 for the Sony cell, 2.19 for the Sanyo cell, and 1.58 for the Panasonic cell. In cycling electrodes from the dissected cells, they found that the end of charge (4.2 V) was reached in the Sony cell due to the change in negative (hard carbon) potential, whereas the Sanyo and Panasonic cells relied on the change in positive ($LiCoO_2$) potential; on discharge, the capacity for all the cells was limited by the negative. The cells were cycled using a 1 C rate charge current to 4.1 V, then an 0.7 C discharge to 40% DOD. The end of discharge voltage (EODV) for the Sony cell decreased almost linearly with cycle number, not reaching the cut-off voltage of 2.7 V even after 4000 cycles. The Panasonic cell exhibited a fairly constant EODV for ~1500 cycles, a linear decline to ~2200 cycles, and then a rapid decrease to the lower voltage limit of 2.7 V at ~2400 cycles. The EODV for the Sanyo cell decreased linearly for the first 1000 cycles, then a greater rate for the next few hundred cycles before hitting the cut-off voltage at ~1500 cycles.

Fellner et al. [14] characterized the performance of 18650-size cells in which the cathode is a mixture of $LiNiO_2$ and $LiCoO_2$ and the anode a mixture of two different carbons, and the electrolyte a mixture of PC, EC and DMC with $LiPF_6$. They found the capacity decreased linearly on cycling at a 1 C rate. Similarly, when cycled at 40% depth of discharge, the EODV decreased linearly with cycle number. Further they found the cell impedance increased linearly with cycle number and the cell impedance increased at a slower rate for cells cycled at 10 °C versus 30 °C. At cycle number 420, the cell impedance (Z) followed an Arrhenius relation ($\ln Z \propto 1/T$) with an activation energy of 63.5 kJ/mol.

Xue et al. [15] found that capacity fade correlated with cell impedance (measured at 1 kHz) for $Li_xMn_2O_4$/graphite cells with a gel electrolyte.

Inoue et al. [16] reported calendar life and cycling results for testing of 100 Ah $LiCoO_2$/Carbon cells. Their calendar life results showed an initial large loss in capacity over the first few months, then the capacity loss was small and varied linearly with time. The calendar life data were used to correct the cycle life results (cycle life capacity loss = observed cycling capacity loss − calendar capacity loss) and the resultant curves of capacity retention versus cycle number were found to overlap, except for the 60 °C results. Further, the corrected cycling capacity loss results were found to correlate linearly with cell internal resistance.

Li et al. [17,18] examined the effects of various charging strategies on commercial lithium-ion cells. First, using Sanyo UF653467 cells, they examined electrodes taken from an uncycled cell and another cell cycled 256× with a proprietary pulse charging method. Based on impedance studies of the cells, and XRD, TEM and SEM studies of the individual electrodes, the authors suggest the fade is due to structural damage of the positive (cracks in the $LiCoO_2$ particles and some loss of interparticle contact) and SEI growth on the negative. A second study with Sony US18650S) cells compared the effect of cycling using a constant current/constant voltage charging protocol to a proprietary pulse charging protocol. Pulse charging reduced charging time and gave higher capacity, but the fade rates appear similar with both charging schemes.

Wang [19] found the capacity fade of $LiCoO_2$ positive active materials from two different manufacturers differed significantly, and argued that this showed capacity fade at the positive was due to chemical transformation of the material rather than loss of electrical contact between particles due to expansion/contraction on cycling.

Kida et al. [20] compared coke, natural graphite, and coke/graphite blends with a $LiCoO_2$ positive in cycle life tests. Their results show a significant reduction in capacity loss using a coke/graphite blend over either material alone. Other authors have reported large improvements in cycle life by use of alternate negative electrode materials such as $Li_{4/3}Ti_{5/3}O_4$ [21]. These results clearly implicate the negative electrode as a major source of capacity fade during cycling.

Bloom et al. [22] reported an accelerated calendar and cycle life study of high-power 18650-size cells with $LiNi_{0.8}Co_{0.2}O_2$/MCMB-6 chemistry. The found the following equation was able to fit their results for each SOC

$$Q = A \exp\left(\frac{-E_a}{RT}\right) t^z \quad (2)$$

where Q represents % increase in impedance or % loss in power, t (weeks) time, T (K) temperature, and A, E_a, and z are adjustable parameters. Adjustable parameter sets (A, E_a, z) were determined for 40, 60, and 80% SOC for the calendar life test (40–70 °C). For the cycle test, parameter sets were obtained at 60 and 80% initial SOC and ΔSOC of 3 and 6% (depth of cycling from initial SOC). For the calendar life tests and for the 3% ΔSOC cycling, the z parameter is ~0.5 indicating a diffusion controlled process; at 6% ΔSOC, the z parameter is much lower (~0.13) suggesting another mechanism takes place. The activation energies and pre-exponential factor are very sensitive to SOC and ΔSOC, except for the good agreement at 40 and 60% SOC in the calendar life test. These results show that the impedance of the cells increases more rapidly with increasing SOC and temperature (calendar test) and with increasing ΔSOC and temperature (cycle test).

Aurbach et al. [23] cycled 18650 cells and then carried out extensive characterization of the electrodes. They found evidence the $LiCoO_2$ positive had degraded. However, they attribute capacity fade to the SEI growth at the positive and negative electrodes. The expansion/contraction of the negative during cycling causes damage to the SEI that must be repaired, and LiF builds up at the positive.

The following summary of experimental data can be made:

(1) Capacity loss on storage has reversible and irreversible components.
(2) Capacity loss on storage or cycling increases with increasing temperature.
(3) Capacity loss on storage increases with increasing cell voltage.
(4) Cycling causes capacity loss at a greater rate than storage.
(5) Capacity loss can correlate with cell impedance.

It is tempting to also conclude that capacity loss on storage reaches a limiting value as this is consistent with all the results reported. However, one must question if calendar life data were available over a period of years, would the capacity curve eventually show a dip, much like the curve for capacity versus cycle number.

Studies of the behavior of individual electrodes provide a more fundamental understanding of capacity fade [24], but the literature is too vast to review here except to mention a few recent studies.

Positive electrode studies have shown that the composition of the active material changes near the surface on cycling [25], that an SEI layer may form at the positive [23,26], and that microstructure of the positive active is damaged on cycling [27], especially at elevated potentials and temperature [28].

Reviews on the SEI growth on the negative are available [29,30]. The work of Zheng et al. [31] is mentioned here because the activation energy for capacity fade of carbon electrodes they report (39.7 kJ/mol) is close to the values reported from the full cell studies discussed earlier.

This literature review suggests that there are at least two major processes relevant to capacity fade: loss of active lithium at the negative and impedance rise at the positive and negative electrodes. Some recent work suggests that there may be interactions between the electrodes.

Wang et al. [32] suggested that acidic impurities generated at the positive electrode can destroy the SEI layer at the negative. This process can be used to explain reversible capacity loss, since the net reaction involves passage of current but could involve no loss of lithium. For example, consider some soluble species, S_1, capable of generating protons at the positive and solvent, S, capable of forming SEI material, LiS.

$$\begin{aligned} &\text{Positive}: \quad S_1 \rightarrow H^+ + e + S_{1a} \\ &\text{Negative}: \quad S + Li^+ + e \rightarrow LiS \\ &\text{SEI}: \quad LiS + H^+ \rightarrow HS + Li^+ \\ &\text{Net}: \quad S_1 + S \rightarrow S_{1a} + HS \end{aligned} \tag{3}$$

Alternatively, Aurbach et al. [23] have suggested that lithiated carbon (perhaps nanoparticles) can actually migrate from the negative to the positive and this causes a reversible capacity loss.

4. Accelerated methods for determination of capacity fade

Time temperature superposition is a well-established method for accelerated testing. The idea is that if a higher temperature accelerates, but does not alter, degradation mechanisms, then the test time can be reduced by testing at higher temperatures. For example, if a 15 °C increase in temperature doubles the rate of degradation, then the time to test the battery is cut in half. This procedure was demonstrated earlier (see Eq. (1)) using Toshiba's calendar life data. Unfortunately, the time acceleration effect achievable by time temperature superposition is bounded by the upper limit on temperature that a cell can be subjected to without changing the degradation mechanism. The literature suggests that earlier 55 °C, the fade mechanism can change. Broussely et al. [33] have applied time temperature superposition for extending calendar life data. Temperature is not the only acceleration factor.

Takei et al. [34] reported a study using Sony 18650-size cells (1.25 Ah) of acceleration factors (charge rate (0.1–1 C), discharge rate (0.1–1 C), ratio of charge/discharge rates (0.1–1), depth of discharge 70–100%), and temperature (10–55 °C)) in cycle life testing. They found that temperature was the most significant factor (reduced test time by >8×), followed by charge rate (reduced test time by >4×), ratio of charge to discharge rates and discharge rate (∼3×), and depth of discharge (∼2×). From their test results, they determined that linear extrapolation of capacity versus cycle number gave at worst ∼40% error.

Majima et al. [21], using charge and discharge current as the acceleration factor, developed the following test for estimating cycle life. The test involves cycling several batteries at different currents. Each battery is charged at a constant current for a fixed time and then discharged to a lower voltage limit at the same current. Plots of the end of charge voltage (EOCV) versus cycle number are linear, and can be extrapolated to 4.0 V to determine the number of cycles to end of life (N_{EOL}). A plot of the $\log(N_{EOL})$ versus current gives a straight line. For example, with a $LiCoO_2$/$Li_{4/3}Ti_{5/3}O_4$ coin cell, they found that at current densities above 1.2 mA/cm^2 the EOCV was reached at 1000 cycles or less. N_{EOL} values extrapolated from lower current densities (such as 0.2 mA/cm^2) were consistent with the N_{EOL} values measured at high current densities, in that a plot of $\log(N_{EOL})$ versus current density was linear. This procedure indicates the cell could deliver >20,000 cycles when cycled at the target current density of 0.2 mAh/cm^2, even though only 1000 cycles were actually measured at 0.2 mA/cm^2.

5. Models for capacity fade

Some purely empirical approaches to predicting capacity fade were described earlier [16,22]. Other authors have

presented models to interpret capacity fade in terms of the physical processes taking place in the cell.

5.1. Irreversible capacity loss due to SEI growth

Broussely et al. [33] posit that capacity fade is due to reaction of lithiated carbon to form SEI and develop a quadratic equation relating capacity fade to time. A slight modification of that derivation, allows accounting for reversible capacity loss. Consider the reaction

$$LiC_6 + S_c \rightarrow LiS_c + C_6 \tag{4}$$

where LiS_c represents lithiated SEI material. Then, a rate expression for SEI formation gives

$$R_f = \frac{dN_{SEI}}{dt} = \frac{k}{Z} = k\frac{a\kappa}{L_0 + N_{SEI}\delta} = \frac{R_{f,0}}{1 + N_{SEI}(\delta/L_0)} \tag{5}$$

where N_{SEI} (%) is the moles of lithiated SEI material divided by the moles of lithium in the negative, t (day) time, R_f (1/day) the rate of SEI formation (the subscript '0' designates the initial rate at $N_{SEI} = 0$), k (Ω/day) a rate constant, Z (Ω) the electronic resistance of the SEI, a (cm^2) the area of the negative, κ (1/(Ω cm)) the specific conductivity, L_0 (cm) the initial thickness of the SEI, and δ (cm) a constant proportional to the molar volume of the SEI material. Integrating with the condition $N_{SEI} = 0$ at $t = 0$, gives

$$t = \frac{D}{2R_{f,0}}N_{SEI}^2 + \frac{1}{R_{f,0}}N_{SEI} \tag{6a}$$

or

$$N_{SEI} = \frac{1}{D}(\sqrt{1 + 2DR_{f,0}t} - 1) \tag{6b}$$

where $D = \delta/L_0$. Eq. (6a) is able to give a reasonable fit (R^2 ~0.86–0.93) to experimental data reported by Broussely et al. [33]. The temperature dependence of the coefficients follows an Arrhenius law with an activation energy for the coefficient of the N_{SEI}^2 square term of ~39 and 37 kJ/mol for the linear term in N_{SEI}. Interestingly, these values are close to the value of 40.5 kJ/mol obtained from linear analysis of the Toshiba data discussed above. Finally, Eq. (5) indicates that the resistance of the SEI, Z, is proportional to the amount of lithiated SEI material and so can be expected to increase with the square root of time.

5.2. Irreversible and reversible capacity loss due to SEI growth

In this section an expression is developed for capacity loss, based on the assumption that the thickness, volume and resistivity of the SEI remains constant, while lithium is liberated by, perhaps, acidic impurities. This liberation of lithium introduces a mechanism for reversible capacity loss. To account for reversible capacity loss, assume that acidic impurities (perhaps electrochemically generated at the positive) react at some rate R_b (%/day) with the SEI as follows:

$$Li_2S + H^+ \rightarrow Li^+ + LiHS \tag{7}$$

Here, in contrast to Eq. (3), the SEI material is taken as involving two lithium ions, one of which can be liberated by acid. Invoking the assumptions the thickness, volume, and resistivity of the SEI are unaffected by liberation of lithium, the following rate expression can be written

$$\frac{dN_{SEI,2}}{dt} = \frac{R_{f,0}}{1 + (N_{SEI,1} + N_{SEI,2})(\delta/L_0)} - \frac{dN_{SEI,1}}{dt} \tag{8}$$

where $N_{SEI,1}$ represents LiHS. This equation can be readily solved for $N_{SEI,2} + N_{SEI,1}$, the solution has the same form as (6) and $N_{SEI,1} = R_b t$. The irreversible capacity loss (measured using a potentiostatic calendar life test) is given by $N_{irr} = 2N_{SEI,2} + N_{SEI,1}$ whereas the total capacity loss (measured using a cell at open-circuit during a calendar life test) is given by $N_{loss} = 2N_{SEI,2} + 2N_{SEI,1}$. The effect of allowing lithium recovery from the SEI by acid is to reduce the irreversible capacity loss at the negative and introduce a reversible capacity loss.

5.3. Irreversible and irreversible capacity loss due to SEI growth and dissolution

Spotnitz [35] considered the effect of the reduction of the thickness of the SEI by acid attack. A simplified analysis is given here. Consider an SEI formation reaction expressed by Eq. (3). The mass balance for lithiated SEI material becomes

$$\frac{dN_{LiS}}{dt} = R_f - R_b \tag{9}$$

The total loss of lithium from the negative (N_{loss}), the irreversible loss (N_{irrs}), and the reversible loss (N_{rev}) are given by

$$N_{loss} = \int R_f\,dt = N_{LiS} + R_b t, \qquad N_{irr} = N_{LiS} + (1-f)R_b t,$$
$$N_{rev} = fR_b t \tag{10}$$

where f represents the fraction of SEI dissolution reaction that liberates lithium.

Integrating Eq. (9) gives a relation for the amount of SEI (expressed in terms of percent of negative capacity)

$$t = \frac{-R_{f,0}}{R_b^2 D}\ln\left(1 - \frac{N_{LiS}}{N_{LiS,st}}\right) - \frac{N_{LiS}}{R_b} \tag{11}$$

where $N_{LiS,st} = (R_{f,0} - R_b)/R_b D$. From Eqs. (10) and (11), the following relation for the total capacity loss derives

$$t = -\left(\frac{R_{f,0} - R_b}{R_b^2 D}\right)\left[1 - \exp\left(-\frac{R_b N_{loss} D}{R_{f,0}}\right)\right] + \frac{N_{loss}}{R_b} \tag{12}$$

The rate of the SEI dissolution should be small relative to the initial rate of the SEI formation reaction, so the above

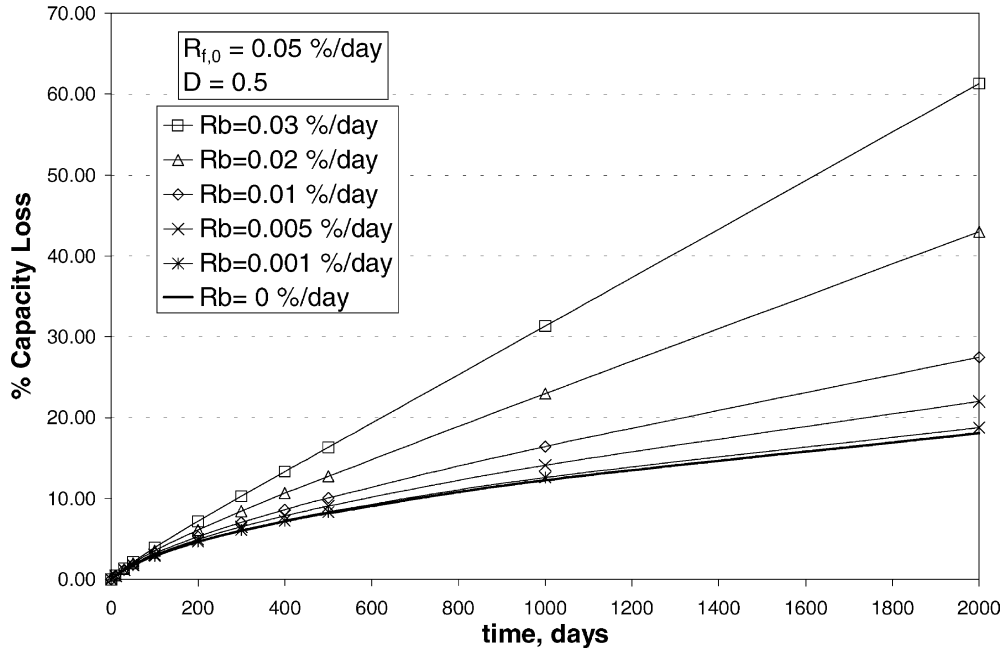

Fig. 4. Effect of SEI dissolution on capacity loss dependence versus time.

equation can be simplified by expanding the exponential term as a quadratic equation and solving for N_{loss}

$$N_{loss} = \frac{R_{f,0}}{(R_{f,0} - R_b)D}\left(\sqrt{1 + 2(R_{f,0} - R_b)Dt} - 1\right) \qquad (13)$$

Note that as $R_b \rightarrow 0$, Eq. (13) reduces to Eq. (6b) (the case of no SEI dissolution reaction).

In this case, SEI dissolution accelerates the rate of new SEI formation. If no lithium is liberated by SEI dissolution ($f = 0$) then $N_{loss} = N_{irr}$, and Fig. 4 shows the effect of the back reaction on capacity loss. If a fraction of the capacity loss can be recovered ($f > 0$), then the irreversible capacity loss can be significantly reduced (see Fig. 5).

The hypothesis of acid attack of the SEI allows reversible capacity loss to be introduced, and provides considerable flexibility in fitting capacity loss versus time curves (see Figs. 4 and 5). Unfortunately, the resultant equations are difficult to use in conjunction with time temperature superposition. In addition, for the cases shown, the differences in capacity loss for times <100 days are relatively small, so life

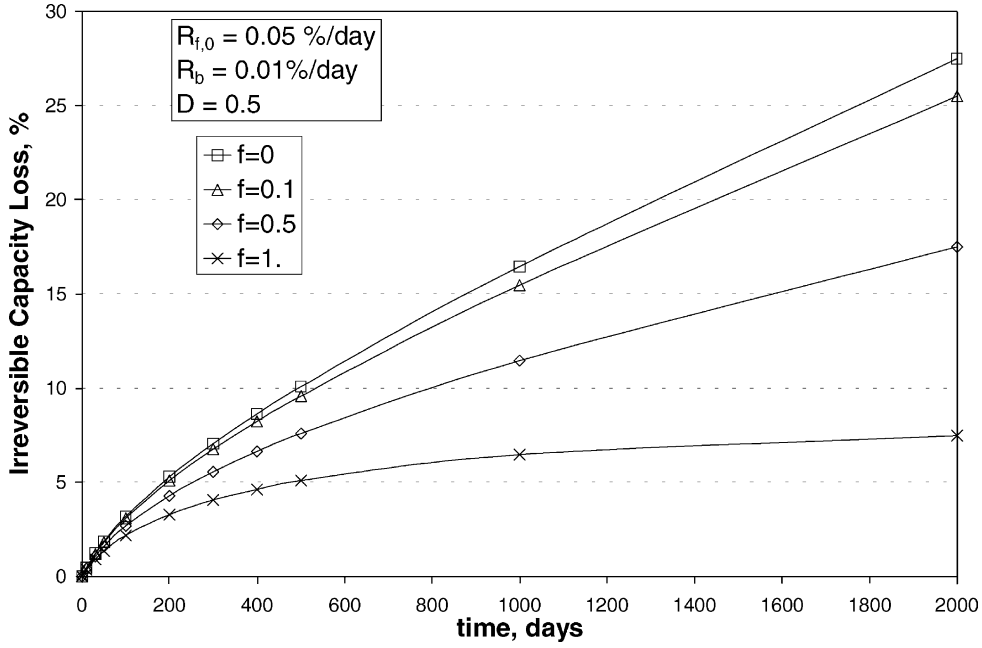

Fig. 5. Effect of Li^+ ion recovery from SEI on irreversible capacity loss.

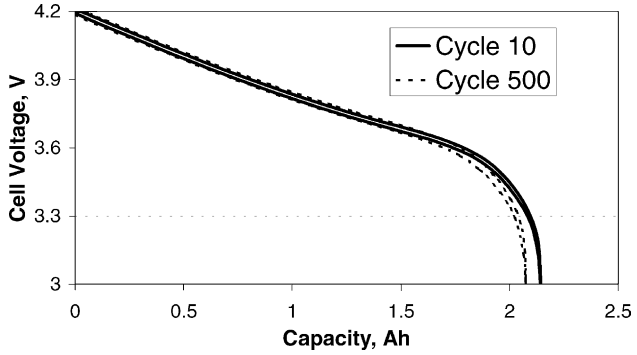

Fig. 6. Simulated cycle test.

testing must be carried out for extended periods to resolve the parameters.

6. Numerical simulation of capacity fade

Numerical simulation must be used in order to account for factors such as the equilibrium voltage curves of actual materials, liquid and solid-phase transport, reaction kinetics, and porous electrodes in prediction of discharge curves. The model developed by Newman's group [36] has proven capable of reproducing the current/voltage/temperature behavior of small lithium-ion cells. This model was modified by including an expression for SEI growth at the negative, and then the model was used to predict the effect of capacity loss at the negative on the cycling behavior of a $LiCoO_2$/graphite cell.

Inclusion of an SEI formation allows voltage/capacity curves such as Fig. 2 to be qualitatively reproduced. However, there is no effect of cycling; cycles taken before and after a calendar life test run at a time equivalent to the cycle life test gives very similar results; see Fig. 6. Under the conditions selected, the concentration and potential gradients that form during cycling are insufficient to enhance the rate of SEI growth. To rationalize the experimental observation that capacity fade depends on charge and discharge rates, it is suggested to take the rate of SEI growth (R_{SEI}) as proportional to the rate of change of surface concentration, that is

$$R_{SEI} = \frac{k_1}{L_{SEI}} + k_2 \left| \frac{\partial c_s}{\partial t} \right| \quad (14)$$

where k_1 and k_2 the are rate constants, L_{SEI} the thickness of the SEI and c_s the concentration of intercalated lithium at the surface of the particle. The basis for this assumption is that the capacity loss is due to disruption of the SEI from expansion/contraction of the active materials, and the rate of expansion/contraction is proportional to the local rate of expansion of the intercalation material.

7. Summary/conclusions

A number of studies have described the capacity fade behavior of lithium-ion cells after storage, and after cycling over a range of temperatures. The results indicate that capacity fade results from at least two major processes: capacity loss due to loss of active lithium at the negative and impedance growth at the positive and negative. There may be an interaction between the positive and negative, as acidic species generated at the positive can attack the SEI at the negative. There is a consensus that limiting the top of charge voltage, significantly reduces capacity fade. If the top of charge voltage is limited to below 4.0 V, simple models for predicting the calendar life of lithium-ion batteries look very promising [16,33]. On the other hand, more work is needed to better understand the impedance rise at the positive. Simulations to predict capacity fade on cycling suggest that the concentration and potential gradients setup in the porous electrodes are insufficient to accelerate fade due to SEI growth. Rather, it is suggested that the rate of SEI growth be equated to the rate of change of lithium concentration at the surface to account for SEI damage by expansion/contraction of the active materials.

Acknowledgements

The author expresses appreciation for NSF Award DMI-0109141 for partial support of this work.

References

[1] http://www.uscar.org/pngv/techtms/eestm.htm.
[2] P. Arora, R. White, M. Doyle, J. Echem. Soc. 145 (10) (1998) 3647.
[3] Y. Wang, M. Zhang, U. von Sacken, B. Way, US Patent 6,045,948 Issued 4 April 2000.
[4] Sony "Technical Information on the Sony Lithium Ion Rechargeable Battery" Brochure from Sony Corporation, 95, 10.
[5] On-line Toshiba Manual, "Storage Characteristics (LG0863448C)" and "Capacity Recovery Rate After Storage", http://www.tbcl.co.jp/TB_e/secondary.htm.
[6] Panasonic Manual, "Lithium Ion Batteries Technical Handbook/Databook", 2000.
[7] F. Beck, P. Ruetschi, Electrochim. Acta 45 (2000) 2467.
[8] http://www.tbcl.co.jp/tb_e/index_e.htm.
[9] B.A. Johnson, R.E. White, J. Power Sources 70 (1998) 48.
[10] S. Tobishima, J. Yamaki, T. Hirai, J. Appl. Electrochem. 30 (4) (2000) 405.
[11] Q. Wu, W. Lu, J. Prakash, J. Power Sources 88 (2000) 237.
[12] D. Zhang, B. Haran, A. Durairajan, R. White, Y. Podrazhansky, B. Popov, J. Power Sources 91 (2000) 122.
[13] A.F. Rakotondrainibe, J.A. Jeevarajan, A.J. Appleby, F.E. Little, in: Proceedings of the 193rd ECS Meeting, San Diego, 7 May 1998.
[14] J.P. Fellner, G.J. Loeber, S.S. Sandhu, J. Power Sources 81–82 (1999) 867.
[15] J. Simon Xue, R.D. Wise, X. Zhang, M.E. Manna, Y. Lu, G. Ducharme, E.A. Cuellar, J. Power Sources 80 (1999) 119–127.
[16] T. Inoue, T. Sasaki, N. Imammura, H. Yoshida, M. Mizutani, NASA Aerospace Battery Workshop, Huntsville, Alabama, 2001.
[17] J. Li, E. Murphy, J. Winnick, P.A. Kohl, J. Power Sources 102 (2001) 294–301.
[18] J. Li, E. Murphy, J. Winnick, P.A. Kohl, J. Power Sources 102 (2001) 302–309.

[19] E. Wang, NASA Aerospace Battery Workshop, Huntsville, Alabama, 2001.
[20] Y. Kida, K. Yanagida, A. Funahashi, T. Nohma, I. Yonezu, J. Power Sources 94 (2001) 74–77.
[21] M. Majima, S. Ujiie, E. Yagasaki, K. Koyama, S. Inazawa, J. Power Sources 101 (2001) 53–59.
[22] I. Bloom, B.W. Cole, J.J. Sohn, S.A. Jones, E.G. Polzin, V.S. Battaglia, G.L. Henriksen, C. Motloch, R. Richardson, T. Unkelhaeuser, D. Ingersoll, H.L. Case, J. Power Sources 101 (2001) 238–247.
[23] D. Aurbach, B. Markovsky, A. Rodkin, M. Cojocaru, E. Levi, H.-J. Kim, Electrochim. Acta 47 (2002) 1–13.
[24] D. Aurbach, J. Power Sources 89 (2000) 206–218.
[25] K. Amine, in: M. Anderman (Ed.), Proceedings of the 1st Adv. Auto. Battery Conf. (AABC-01); February 2001.
[26] S.S. Zhang, K. Xu, T.R. Jow, Electrochem. Solid-State Lett. 5 (5) (2002) A92–A94.
[27] H. Wang, J.-I. Jang, B. Huang, D.R. Sadoway, Y.-M. Chiang, J. Electrochem. Soc. 146 (2) (1999) 473–480.
[28] K. Dokko, S. Horikoshi, T. Itoh, M. Nishizawa, M. Mohamedi, I. Uchida, J. Power Sources 90 (2000) 109–115.
[29] E. Peled, D. Golodnitsky, J. Pencier, in: J.O. Besenhard (Ed.), Handbook of Battery Materials, Wiley, New York, 1999.
[30] D. Aurbach, B. Markovsky, I. Weissman, E. Levi, Y. Ein-Eli, Electrochim. Acta 45 (1999) 67–86.
[31] T. Zheng, A.S. Gozdz, G.G. Amatucci, J. Electrochem. Soc. 146 (1999) 4014–4018.
[32] E. Wang, D. Ofer, W. Bowden, N. Iltchev, R. Moses, K. Brandt, J. Electrochem. Soc. 147 (2000) 4023–4028.
[33] M. Broussely, S. Herreyre, P. Biensan, P. Kasztejna, K. Nechev, R.J. Staniewicz, J. Power Sources 97–99 (2001) 13–21.
[34] K. Takei, K. Kumai, Y. Kobayashi, H. Miyashiro, N. Terada, T. Iwahori, T. Tanaka, J. Power Sources 97–99 (2001) 697–701.
[35] R. Spotnitz, in: M. Anderman (Ed.), Proceedings of the 2nd Adv. Auto. Battery Conf. (AABC-02); February 2002.
[36] T.F. Fuller, M. Doyle, J. Newman, J. Electrochem. Soc. 141 (4) (1994) 962–990.